EFFECTS OF ASH CONTENT AND CURING TIME ON COMPRESSIVE STRENGTH OF CEMENT PASTE WITH RICE HUSK ASH

Sitthisak Prasanphan, Samunya Sanguanpak, Supaporn Wansom*, and Thammarat Panyathanmaporn

Received: May 19, 2010; Revised: Jul 15, 2010; Accepted: Jul 16, 2010

Abstract

This research investigates the effect of ash content and curing time on the compressive strength and microstructural development of cement pastes blended with rice husk ash (RHA). To explore the use of RHA obtained from a typical biomass power plant as a supplementary cementitious material, plain Type I ordinary Portland cement (OPC) paste and OPC pastes with 5 and 25 wt% RHA were cast and tested for compressive strength at 1, 7, and 28 days of curing. Scanning electron microscopy (SEM) study and thermogravimetric/differential thermal analysis (TG/DTA) were used to follow the microstructural development and the extent of hydration and pozzolanic reactions of the pastes, respectively. The compressive strengths of all pastes were found to increase with curing time. The OPC+5%RHA paste exhibited higher compressive strengths than the plain OPC paste only after 7 days of curing, while the OPC+25%RHA paste only showed lower compressive strengths than the plain OPC paste at all curing times. The higher compressive strength was supported by the greater growth and concentration of the ettringite needles in the SEM micrographs. The extents of cement hydration reaction and pozzolanic reaction in relation to strength development are discussed based on the $Ca(OH)_2$ content from TG/DTA.

Keywords: Rice husk ash, Pozzolanic activity, Compressive strength, Blended cement paste

Introduction

Rice husk is the one of the most abundant agricultural wastes in Thailand. When it is properly burnt at a temperature below 800ºC, rice husk ash (RHA) with cellular microstructure and high percentage of amorphous SiO_2 is produced. The resulting RHA is very suitable for use as a pozzolanic material to improve the compressive strength and durability of

---

National Metal and Materials Technology Center, 114 Thailand Science Park, Phahonyothin Rd., Klong 1, Klong Luang, Pathumthani 12120. Tel: 0 2564 6500 ext. 4042, Fax: 0 2564 6368, E-mail: supaporw@mtec.or.th
* *Corresponding author*

cement-based materials (Zhang *et al.*, 1996; Nair *et al.*, 2006). Many studies have found that the compressive strengths of cement paste or mortar blended with RHA depend on many factors such as the extent of cement hydration reaction (Yu *et al.*, 1999), the content, and particle size of the RHA (Rukzon *et al.*, 2009). The ability of RHA to act as a pozzolan comes from two sources. Firstly, the fine RHA particles (preferably finer than the median cement particle size of ~10 μm) can arrange to physically fill in the voids between adjacent cement particles, thus reducing the porosity and/or increasing the packing density of the material. Consequently, the material's compressive strength and durability are improved through this so-called filler effect. Secondly, it can act as a source of excess SiO_2 to chemically react with $Ca(OH)_2$, a product from cement hydration (Equations 1 and 2), to form additional calcium silicate hydrate (approximate formula: $3CaO{\cdot}2SiO_2{\cdot}8H_2O$ or CSH), the compound responsible for strength in cement-based materials (EEquation 3). This so-called pozzolanic effect is especially pronounced in RHA with a high content of amorphous SiO_2, which is the most chemically reactive form of SiO_2 to $Ca(OH)_2$.

Hydration reactions of calcium silicates in cement (Mindess et al., 2003):

$$2(3CaO{\cdot}SiO_2) + 11H_2O \rightarrow 3CaO{\cdot}2SiO_2{\cdot}8H_2O + 3Ca(OH)_2 \quad (1)$$

$$2(2CaO{\cdot}SiO_2) + 9H_2O \rightarrow 3CaO{\cdot}2SiO_2{\cdot}8H_2O + Ca(OH)_2 \quad (2)$$

Pozzolanic reaction (Mindess et al., 2003):

$$3Ca(OH)_2 + 2SiO_2 + 5H_2O \rightarrow 3CaO{\cdot}2SiO_2{\cdot}8H_2O \quad (3)$$

However, most rice husk in Thailand is typically burnt at temperatures in excess of 1000°C in a boiler for biomass power plants. Such high temperatures, coupled with prolonged incineration times, can cause a major portion of the amorphous SiO_2 to phase-transform to cristobalite, the crystalline and less reactive form of SiO_2, thus weaken the pozzolanic property of the RHA. To explore the use of RHA obtained from a typical biomass power plant as a pozzolanic material, this research investigates the strength development of cement paste blended with 5 and 25 wt% RHA as a function of curing time. The compressive strengths of the blended pastes at curing times of 1, 7, and 28 days will be discussed in relation to the microstructural development and the extent of the hydration and pozzolanic reactions, as examined by scanning electron microscopy (SEM) and thermogravimetric/differential thermal analysis (TG/DTA), respectively. Results of plain cement paste made to achieve a similar flow will also be discussed in comparison.

Materials and Methods

The RHA collected from a biomass power plant in Ang-Thong was used to partially replace Type I ordinary Portland cement (OPC) in this work. The particle size distributions of the OPC and RHA were determined by laser diffraction technique (Mastersizer S, Malvern Instrument, UK), while their chemical compositions were examined by X-ray fluorescence (XRF, PW 2404, 4 kW, Phillips, Netherlands). The specific surface areas of both powders were measured by nitrogen adsorption (Autosorb-1, Quanta Chrome, USA) after the samples were outgassed at 300°C for 6 hours. A scanning electron microscope (SEM, JSM-5401, JEOL, Japan) and an X-ray diffractometer (XRD, JDX 3530, JEOL, Japan) were also used to investigate the microstructure and crystalline phases of the RHA prior to mixing with the OPC, respectively.

The conductometric method developed by Luxán *et al.* (1989) was adopted to preliminarily assess the pozzolanic activity of the RHA. The method measures the conductivity drop after 5 g of the RHA was added to 200 ml saturated $Ca(OH)_2$ solution as a result of the consumption of Ca^{2+} and OH^- ions by the pozzolanic reaction. Therefore, the faster the conductivity drops, the better is the pozzolanic activity. The measurements were made every 0.5-1 min for 1 hour at 40°C under constant stirring using a portable conductivity meter (PC 300 series, Oakton Instruments, Singapore) with a cell constant, k, of 1.0 cm^{-1}. The conductivity values compensated at 25°C (using a temperature coefficient of 0.021/°C) are reported, to eliminate the effect of temperature on conductivity. According to the work of Luxán *et al.* (1989), the conductivity change during the first 2 min, $\Delta\sigma$ (mS/cm) , allowed a broad classification of natural rock pozzolans into three groups, non pozzolanicity ($\Delta\sigma < 0.4$), variable pozzolanicity ($0.4 \leq \Delta\sigma \leq 1.2$), and good pozzolanicity ($\Delta\sigma > 1.2$). To support the conductivity result, the amorphous SiO_2 content of the RHA was measured by a chemical extraction method proposed by Payá *et al.* (2001). It was determined from the weight loss of the RHA sample after being washed in a boiling 4 M KOH solution for 3 min.

Plain OPC paste, and OPC pastes with 5 and 25 wt% RHA (by weight of total binders, the binders being OPC and RHA) were made with different water/binders ratios of 0.30, 0.31, and 0.47, respectively, following the mixing procedures in ASTM C109 (2002). The ratios were used in order to maintain a constant flow of 110 ± 5% for each mix during casting, as determined by a flow table test according to ASTM C230 (2003). The specimens were cast into 50 mm × 50 mm × 50 mm cubes and cured at 23 ± 2°C for 24 hours. After demolding, the specimens were stored in a saturated calcium hydroxide solution at 23 ± 2°C for 1, 7, and 28 days. The test for compressive strength was conducted at these three different ages in accordance with ASTM C109 (2002) using a loading rate of 1.5 mm/min, with the reported compressive strength being an average of three specimens. A different set of specimens were cast in order for the reaction products to be examined via SEM and the $Ca(OH)_2$ contents determined by TG/DTA (Simultaneous Thermal Analysis, STA 449C, NETZSCH, Germany), both as a function of curing time. For the estimation of the $Ca(OH)_2$ contents, the temperature ranges over which the decompositions of $Ca(OH)_2$ occurred were determined from a dip in the DTA curve (in the range 400-550°C, depending on the different pastes). Then, the weight losses due to such decompositions were determined from the TG curve. The weight losses were due to the loss of water as $Ca(OH)_2$ decompose into CaO and H_2O, therefore the initial content of the $Ca(OH)_2$ can be stoichiometrically calculated. For a more careful estimation, the $Ca(OH)_2$ contents were calculated with respect to the final ignited weight of the pastes at 1000°C.

Results and Discussion

The average size of the OPC particles (15.14 ± 0.09 μm) is finer than that of the RHA (28.71± 0.06 μm), as determined from the particle size distribution in Figure 1. This difference is confirmed by the SEM micrographs in Figures 2 and 3 for the RHA and the OPC powders, respectively. The BET specific surface areas are 12.67 ± 0.10 m^2/g for the RHA and 2.58 ± 0.35 m^2/g for the OPC. Despite the coarser particles, the RHA still exhibits many times greater specific surface area than the OPC due to its microporous structure as evident in Figure 2 (c).

The chemical oxide compositions of the OPC and RHA are shown in Table 1. The main chemical components of the OPC are CaO, SiO_2, Al_2O_3, Fe_2O_3, and SO_3. The RHA is composed of as high as 93.86 wt% SiO_2, with some minor amounts of other oxides. However, this number includes not only amorphous SiO_2 but also crystalline SiO_2 (i.e., cristobalite and quartz as shown in the XRD profile of Figure 4) in the RHA. By chemical extraction, it is found that the RHA contains only 27.58 wt% of amorphous SiO_2. This is especially low compared with conventional pozzolans such as silica fume and fly ash, whose amorphous SiO_2 contents are typically in excess of 85 wt%. However, the result is not unexpected, given the high incineration temperature adopted in typical biomass power plants. The low amorphous SiO_2 content of the RHA is further confirmed by the conductivity drop of only 0.04 mS/cm after 2 min of RHA addition to the saturated $Ca(OH)_2$ solution. This slight conductivity drop puts the RHA investigated in this work under the "non-pozzolanicity" category, according to Luxán *et al.* (1989). As evident in Figure 5, even at 60 min after the RHA addition, the conductivity drop is still less than 0.2 mS/cm, signifying that the RHA is essentially inert.

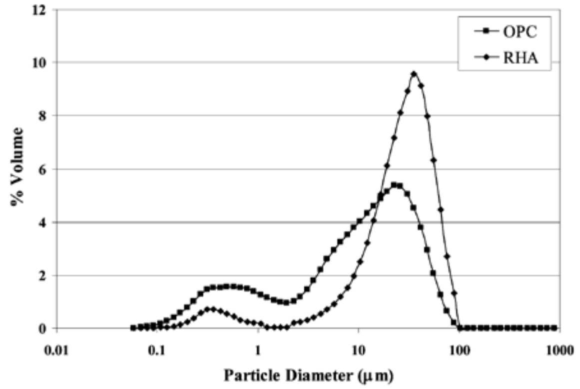

Figure 1. Particle size distributions of the OPC and RHA

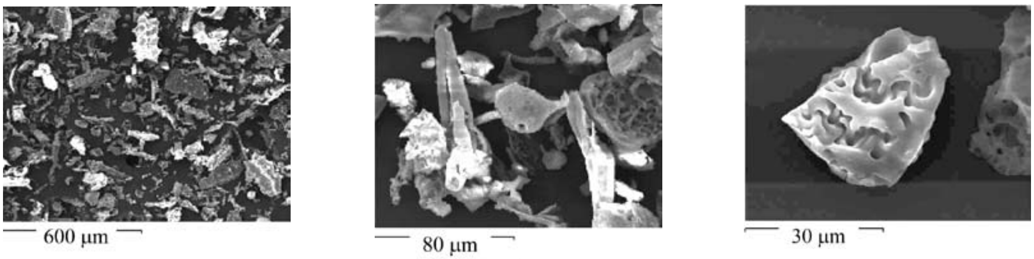

(a) (b) (c)

Figure 2. SEM micrographs of RHA at (a) 100X, (b) 750X, and (c) 2000X magnifications

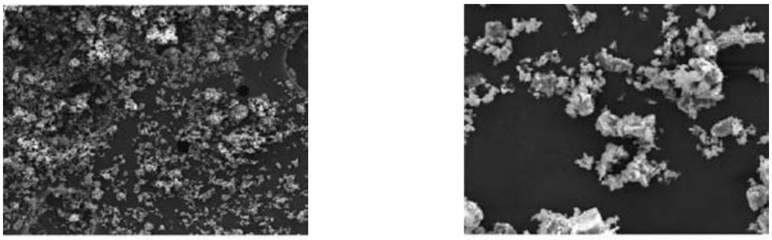

(a) (b)

Figure 3. SEM micrographs of OPC at (a) 100X and (b) 750X magnifications

Table 1. Chemical oxide compositions of the OPC and RHA

Oxides (wt%)	OPC	RHA
SiO_2	21.63	93.86
Al_2O_2	5.10	0.21
MgO	1.06	0.40
P_2O_5	0.08	0.60
SO_3	2.25	0.03
K_2O	0.5	1.70
CaO	64.01	0.59
MnO	0.05	0.09
Fe_2O_3	2.88	0.19
CuO	0.03	0.01
TiO_2	0.23	-
SrO	0.02	-
Cr_2O_3	0.02	-

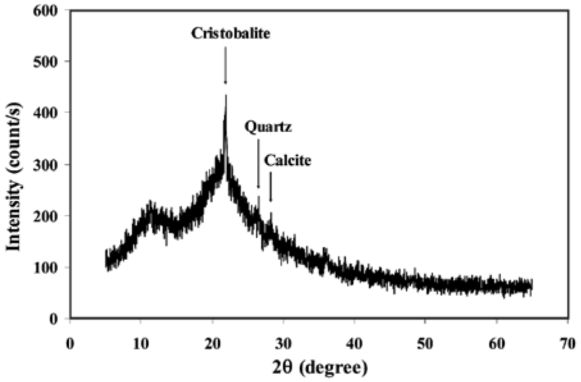

Figure 4. XRD profile of RHA with evidence of crystalline phases of SiO_2 (cristobalite and quartz)

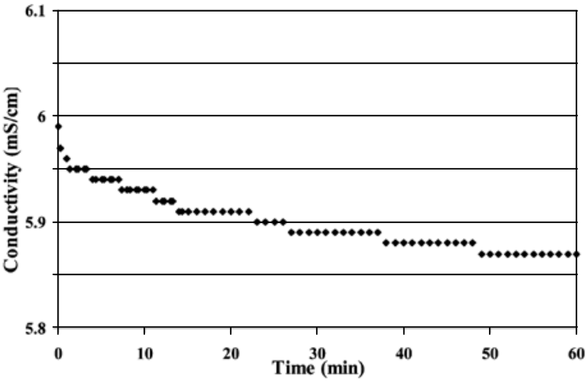

Figure 5. Conductivity vs. time of the RHA + $Ca(OH)_2$ solution

To maintain a constant flow of 110 ± 5% for each mix according to ASTM C109 (2002), the mix proportions in Table 2 were used. As expected, the water requirement of the pastes increases with the dosage of RHA replacement due to the porous structure, and thus the greater water absorption of the RHA. This effect was also observed by Rukzon *et al.* (2009). The resulting compressive strengths of the pastes at different curing times are represented in Figure 6. Apparently, the compressive strengths for all pastes increase with curing time. As the pastes were allowed to hydrate longer, cement hydration reaction proceeded to a greater extent, resulting in a larger amount of the reaction products. This leads to reduced porosity and thus enhanced compressive strength as the curing time increases for all pastes.

This explanation is supported by the $Ca(OH)_2$ content which steadily increases with the curing time for a given paste, as shown in Figure 7. The increase seems to slow down at longer curing times due to the slowing down of the hydration reaction. The fact that such a slowing down is more noticeable in the pastes with greater RHA additions might be primarily owing to the dilution effect (i.e., a greater amount of cement was replaced with RHA, thus reducing the $Ca(OH)_2$ content from cement hydration) and slightly, if at all, to the pozzolanic effect (i.e., more $Ca(OH)_2$ is consumed in the pozzolanic reaction with more RHA).

Microstructural investigation in the cavity of the pores, as shown in Figure 8, reveals the growth of ettringite crystals, one of the cement hydration products, as the

Table 2. Mix proportions of the pastes with different RHA replacements

SPECIMEN	Water/Binders Radio	Flow (%)
OPC	0.30	109
OPC + 5% RHA	0.31	112
OPC + 25% RHA	0.47	111

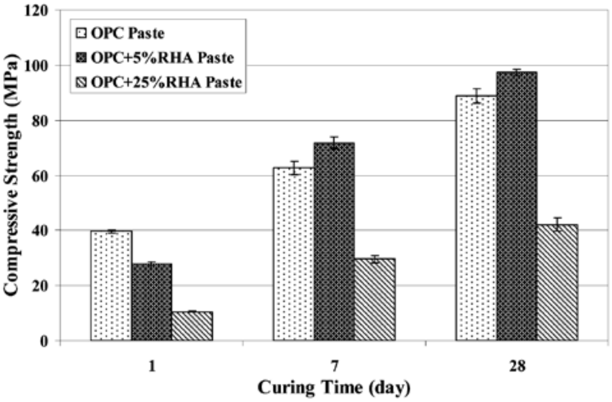

Figure 6. Compressive strength vs. curing time for the different pastes

curing time increases for all pastes, supporting the explanation that the improved compressive strength and the steady increase in the $Ca(OH)_2$ content as the curing time increases for each of the pastes are due to the greater extent of hydration. Ettringite ($3CaO \cdot Al_2O_3 \cdot 3(CaSO_4) \cdot 32H_2O$) results from hydration of tricalcium aluminate in cement, which involves the reactions with sulfate ions supplied by dissolution of gypsum and water, as shown in Eq. 4.

Hydration reactions of calcium aluminate in cement (Mindess et al., 2003):

$$3CaO \cdot Al_2O_3 + 3[CaSO_4 \cdot 2H_2O] + 26H_2O \rightarrow 3CaO \cdot Al_2O_3 \cdot 3CaSO_4 \cdot 32H_2O \quad (4)$$

It is generally observed as long slender needles as shown in Figure 9, with the energy-dispersive spectrum (EDS) showing Ca, Al, and the characteristic S contents of ettringite. Comparing at the same curing time of 1 day, the compressive strength shows a decrease with greater RHA addition. Since the $Ca(OH)_2$ contents of the three pastes are very similar at 1 day, suggesting limited or no extent of the pozzolanic reaction at such an early time, the reduction in compressive strength is more likely be explained by the greater dilution effect accompanying the higher RHA addition, i.e., the greater replacement of cementitious binder with an inert filler (even of a larger particle size in this case). However, although it may already affect the pastes mechanically, the dilution effect might not yet be realized chemically, in terms of the decreased $Ca(OH)_2$ content, at such a very early curing time as 1 day when hydration products still continue to form. The micrographs in Figure 8 reveal that the ettringite needles seem to grow finer as the RHA addition increases. This reduction in size of the ettringite crystals might be a direct microstructural consequence of the dilution effect, which essentially acts to lower the compressive strength.

At 7 and 28 days, the OPC+5% RHA paste exhibits higher compressive strength than the plain OPC paste; the differences are about 14% and 10%, respectively. The OPC+ 25% RHA paste, however, displays roughly 53% lower compressive strength than the plain OPC paste at both 7 and 28 days of curing. For the OPC+5%RHA paste, the improved compressive strength relative to the plain OPC paste at 7 and 28 days cannot be mainly due to the pozzolanic effect, because of the low amorphous SiO_2 content and the essentially inert nature of the RHA. It is also unlikely that the RHA, whose mean particle size is almost twice that of the cement particles, can positively contribute to increase the paste's

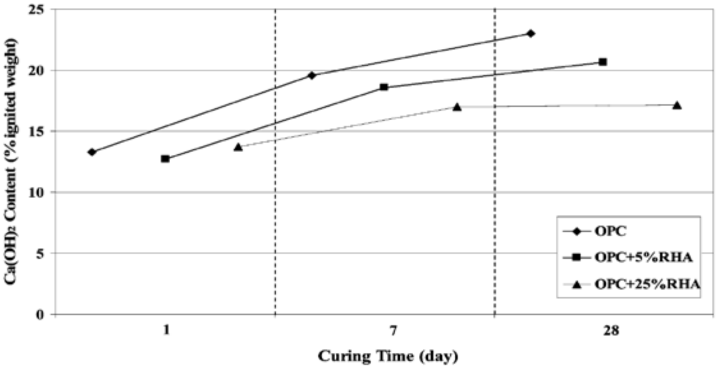

Figure 7. $Ca(OH)_2$ content o f the pastes as a function of curing time

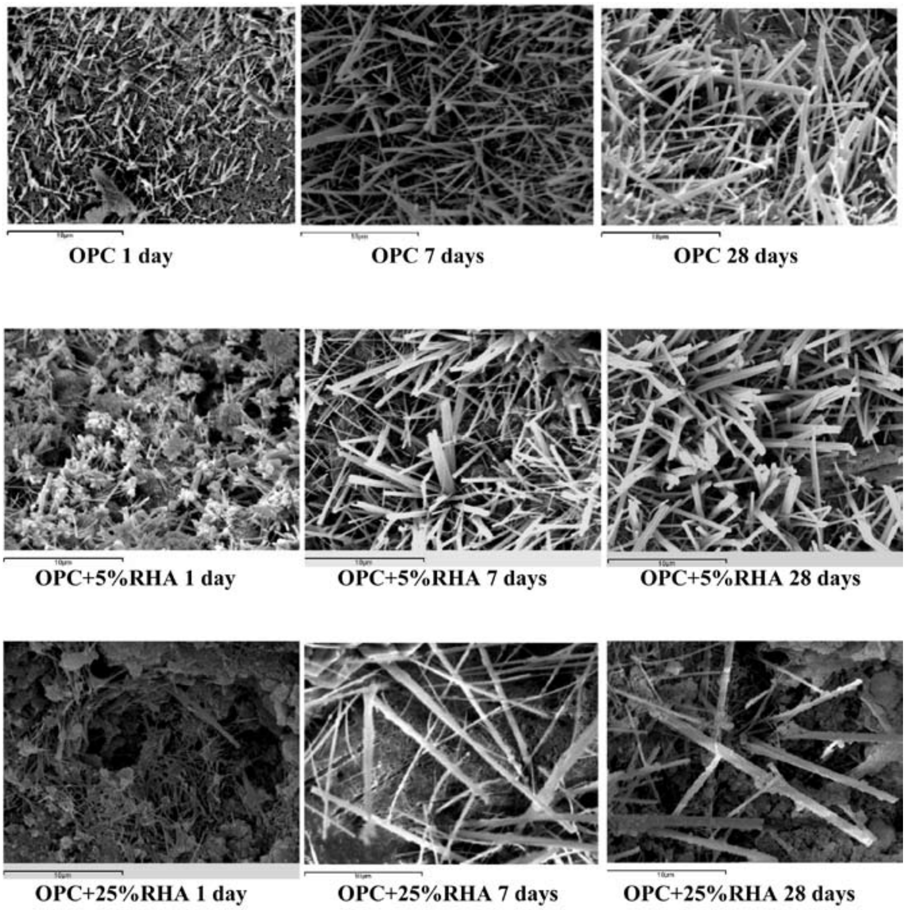
OPC 1 day
OPC 7 days
OPC 28 days
OPC+5%RHA 1 day
OPC+5%RHA 7 days
OPC+5%RHA 28 days
OPC+25%RHA 1 day
OPC+25%RHA 7 days
OPC+25%RHA 28 days

Figure 8. SEM micrographs at 5000X magnification of the three pastes at different curing times (all scaling bars correspond to 10 µm)

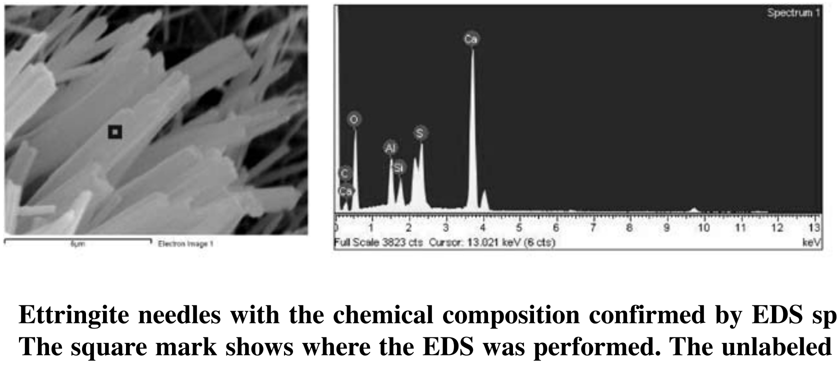

Figure 9. Ettringite needles with the chemical composition confirmed by EDS spectrum. The square mark shows where the EDS was performed. The unlabeled peak to the right of 2 keV in the EDS spectrum corresponds to Au used for sample preparation.

compressive strength through the filler effect. The dilution effect, if any, will only act to *decrease* the compressive strength of the OPC+5%RHA paste compared with that of the plain OPC paste, although the effect is expected to be minor due to the small RHA addition of only 5%. From the examination of Figure 8, it is interesting to note that the ettringite needles in the OPC+5%RHA paste are larger than in the plain OPC paste, both at 7 and 28 days, (the difference is more pronounced at 7 days). The growth of ettringite seems to be accelerated by the presence of 5 wt% RHA, possibly due to the greater amount of porosity or the improved hydration conditions (e.g., a larger amount of water) accompanying the RHA addition. Although the origin of this accelerated ettringite growth is still unclear, its existence may partly help explain the superior compressive strength of the OPC+5%RHA paste compared with the plain OPC paste at 7 and 28 days. With the possibility of the pozzolanic effect being ruled out, the slight reduction in the $Ca(OH)_2$ content at 7 and 28 days of the OPC+5% RHA paste from that of the plain OPC paste should, therefore, be primarily due to the dilution effect.

For the OPC+25% RHA paste, the reduced compressive strength compared with that of the plain OPC paste at 7 and 28 days is mainly due to the dilution effect (lower amount of cementitious binder), as accompanied by the lower $Ca(OH)_2$ content and lower concentrations of the ettringite crystals compared with the plain OPC paste as shown in Figure 8. The considerable drop in compressive strength of the pastes as the RHA replacement was increased from 5% to 25% might further be explained by the difference in homogeneity of the RHA dispersion between the two pastes. Gemelli *et al.* (2004) proposed that areas with high concentrations of inert particles may impede the nucleation of ettringite. In our case, the higher RHA concentration in the OPC+25% RHA paste may make it more susceptible to agglomeration problems, leading to greater inhibition of ettringite growth, higher porosity, and thus lower compressive strength than the OPC+5% RHA paste.

Conclusions

The origins of the change in compressive strengths of OPC pastes blended with 5% and 25% RHA at different curing times of 1, 7, and 28 days were investigated. The compressive strength gain with curing time for each paste was primarily due to further extent of hydration, as confirmed by the $Ca(OH)_2$ content and the SEM micrographs. At 1 day, the compressive strength of the pastes was found to decrease systematically with the increased RHA addition, as a result of the dilution effect. At 7 and 28 days, the OPC+5% RHA exhibited the highest compressive strength, followed by the plain OPC paste and the OPC+25% RHA paste, respectively. The increase in compressive strength of the OPC+5% RHA paste at 7 and 28 days could not be reasoned by the pozzolanic effect because of the very low pozzolanic activity of the RHA. From microstructural examination, however, it was evident that the essentially inert RHA may play some roles in accelerating the growth of ettringite, hence partly increasing the strength of the OPC+5% RHA paste at 7 and 28 days. The reduced compressive strengths of the OPC+25% RHA paste with respect to the plain OPC paste at 7 and 28 days were most likely to be explained by the dilution effect. In addition to these effects, the vast difference in compressive strength of the OPC+5% RHA and the OPC+25% RHA pastes might also be reasoned by the different homogeneity of the RHA dispersion in these two pastes.

References

ASTM C109/C109M-02 (2002). Standard Test Method for Compressive Strength of Hydraulic Cement Mortars. In: Annual Book of ASTM Standard. ASTM International, West Conshohocken, PA, USA, p. 76-81.

ASTM C230/C230M-03 (2003). Standard Specification for Flow Table for Use in Tests of Hydraulic Cement. In: Annual Book of ASTM Standard. ASTM International, West Conshohocken, PA, USA, p. 206-211.

Gemelli, E., Cruz, A.A.D.F., and Camargo, N.H.A. (2004). A study of the application of residue from burned biomass in mortars. Materials Research, 7(4): 545-556.

Luxán, M.P., Madruga, F., and Saavedra, J. (1989). Rapid evaluation of pozzolanic activity of natural products by conductivity measurement. Cement and Concrete Research, 19(1): 63-68.

Mindess, S., Young, J.F., and Darwin, D. (2003). Concrete. 2nd ed. Prentice Hall, Upper Saddle River, NJ, USA, 644p.

Nair, D.G., Jagadish, K.S., and Fraaij, A. (2006). Reactive pozzolanas from rice husk ash: An alternative to cement for rural housing. Cement and Concrete Research, 36(6): 1062-1071.

Payá, J., Monzó, J., Borrachero, M.V., Mellado, A., and Ordoñez, L.M. (2001). Determination of amorphous silica in rice husk ash by a rapid analytical method. Cement and Concrete Research, 31(2): 227-231.

Rukzon, S., Chindaprasirt, P., and Mahachai, R. (2009). Effect of grinding on chemical and physical properties of rice husk ash. International Journal of Minerals, Metallurgy and Materials, 16(2): 242-247.

Yu, Q., Sawayama, K, Sugita, S., Shoya, M., and Isojima, Y. (1999). The reaction between rice husk ash and $Ca(OH)_2$ solution and the nature of its product. Cement and Concrete Research, 29(1): 37-43.

Zhang, M.H., Lastra, R., and Malhotra, V.M. (1996). Rice-husk ash paste and concrete: Some aspects of hydration and the microstructure of the interfacial zone between the aggregate and paste. Cement and Concrete Research, 26(6): 963-977.